Using EXAFS for the structural characterization of MoO$_3$ rods and their synthesis

J.-D. Grunwaldt, G. R. Patzke[1], R. Nesper[1], and A. Baiker

*Laboratory of Technical Chemistry, ETH Hönggerberg - HCI, CH-8093 Zürich, Switzerland*

[1]*Laboratory of Inorganic Chemistry, ETH Hönggerberg - HCI, CH-8093 Zürich, Switzerland*

The controlled synthesis of nanoparticles is interesting in a number of fields, such as nanotechnology and catalysis [1]. Among the multitude of newly generated nanomaterials, oxidic nanorods are especially valuable, because they combine a distinct anisotropic morphology with the manifold important properties of oxidic materials. In addition, materials like molybdenum oxides and mixed molybdenum oxides are well-known catalysts for reactions, such as methanol oxidation and selective oxidation of alkenes [2-4].

Recently, the solvothermal synthesis of MoO$_3$ nanorods has been studied and optimised. A convenient "one-pot-procedure" has been developed that gives controlled access to MoO$_3$ rods in gram-scale quantities. This experimental routine can be tuned by varying parameters such as solvent system and temperature in order to tailor the size and shape of the rod-shaped products. The crucial step during each procedure of rod formation is always the dehydration of the starting material, MoO$_3$·2H$_2$O, to give MoO$_3$. Mechanistic investigations have been performed to gain further insights and control facilities, and the underlying reaction pathways of the tailor-made syntheses turned out to be both different from each other and from the dehydration mechanism observed under ambient conditions [5]. XAFS is an important tool because it monitors both the crystalline and amorphous phases in these systems. Some XAFS studies have recently been reported on the redox behaviour of MoO$_3$ and on the dehydration reactions of molybdenum trioxide hydrates [4,6]. Therefore, we have employed this technique to characterize several types of MoO$_3$ rods and the intermediates leading to them.

Mo K-edge EXAFS data were recorded in the transmission mode at station X1 (DORIS III operating at 4.4 GeV, injection current 140 mA, Si(311)-double-crystal monochromator). For this purpose ca. 40-80 mg of the samples were pressed to self-supporting wafers. Energy calibration was performed with a molybdenum foil (first inflection point at 20,000 eV). The spectra were energy corrected, background subtracted and normalized. After conversion into k-space the EXAFS signals were extracted and Fourier transformed.

The MoO$_3$ rods were prepared in the following way: In a standard procedure, the hydrothermal reaction of MoO$_3$·2H$_2$O was performed in an autoclave at 180°C for 2 – 6 d in the presence of diluted glacial acetic acid. Filtering and washing with ethanol and water resulted in the metallic-blue MoO$_3$ nanorod material. A typical SEM picture of MoO$_3$ nanorods is shown as an example in Figure 1. In the first part of the EXAFS studies, different MoO$_3$ nanonods were compared to references, such as MoO$_3$ and MoO$_3$·2H$_2$O. The results are shown in Figure 1. It is obvious that the structure is similar to MoO$_3$. While the first shell at about 1.5 Å is due to Mo-O, the second shell at 3.5 Å can be contributed to molybdenum neighbours. The samples are thus completely dehydrated. Whereas the macrostructure is very different, the microstructure is quite similar. Small variations
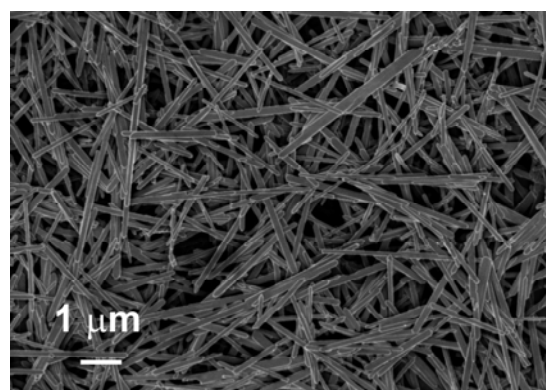

Figure 1: Representative SEM image of MoO$_3$ rods

can be found in the intensity of the Mo-O and Mo-Mo backscattering. These are probably due to small variations in the structure and could be caused by the thickness of the nanorods (decrease of the peaks leads to a decrease in the backscattering).
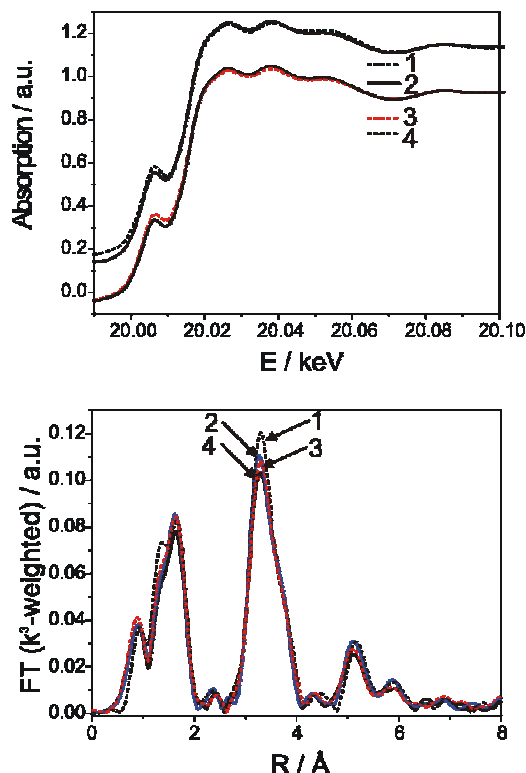
Figure 2: Mo K-EXAFS spectra and the corresponding Fourier transforms: (1) MoO_3 (2-4) nanorods with decreasing rod diameter (see text).
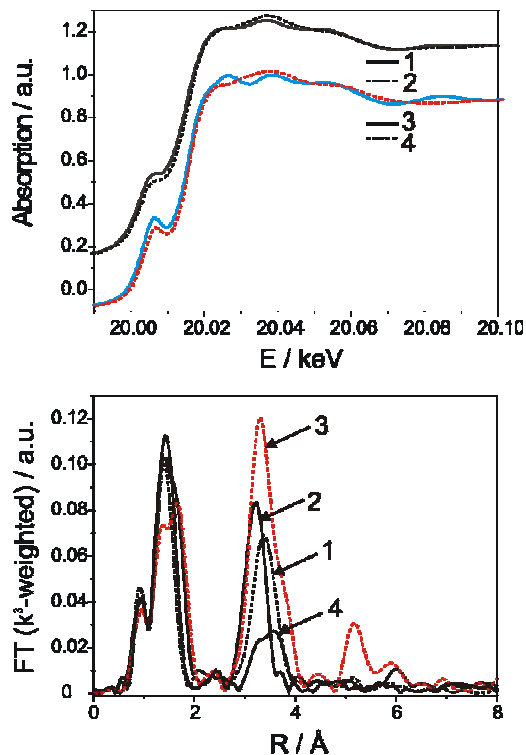
Figure 3: Mo K-EXAFS spectra and corresponding Fourier transforms: (1) α-$MoO_3 \cdot H_2O$, (2) $MoO_3 \cdot 1/3H_2O$, (3) MoO_3 and (4) $MoO_3 \cdot 2H_2O$

In the second part of the EXAFS studies samples were selected that correspond to intermediates of the synthesis: Both α-$MoO_3 \cdot H_2O$ and $MoO_3 \cdot 1/3H_2O$ (phases were identified by X-ray diffraction) are compared to reference samples in Figure 3. The first Mo-O shell is significantly increased compared to MoO_3 and thus shows that the molybdenum is in similar coordination as in $MoO_3 \cdot 2H_2O$. However, the backscattering of the second Mo-shell is significantly higher than in the layered $MoO_3 \cdot 2H_2O$ structure. The loss of interlayer water molecules from the $MoO_3 \cdot 2H_2O$ leads to layers of edge-sharing $[MoO_5(H_2O)]$ octahedra connected by hydrogen bonds in α-$MoO_3 \cdot H_2O$ [7]. $MoO_3 \cdot 1/3H_2O$ is made up of infinite planes of MoO_3 octahedra sharing their corners to form six-membered rings that are subsequently layered [5]. So the three-dimensional character of the Mo-O framework increases with decreasing water content and can be interpreted with respect to the changing Mo-O-Mo angle in these structures.

References

[1] G. R. Patzke, F. Krumeich, R. Nesper, *Angew. Chem.* 41, 2447 (2002).

[2] A. Baiker, D. Gasser, *Z. Phys. Chem.*, 149, 119 (1986).

[3] B. Grzybowska-Swierkosz, *Topics Catal.* 11, 23 (2000)

[4] T. Ressler, J. Wienold, R. E. Jentoft, T. Neisius, *J. Catal.* 210, 67 (2002); T. Ressler, O. Timpe, T. Neisius, J. Find, G. Mestl, M. Dieterle, R. Schlögl, *J. Catal.* 191, 75 (2000).

[5] M. Figlarz, *Prog. Solid St. Chem.* 19, 1 (1989)

[6] A. Kuzmin, J. Purans, *J. Phys.: Condens. Matter* 12, 1959 (2000).

[7] I. Böschen, B. Krebs, *Acta Cryst.* B30, 1795 (1974).